

Effects of Nitrate Fertilization on Pyrite Oxidation in Salt Marsh Sediments

Ben Pyenson¹

Advisor: Dr. Anne Giblin²

¹ Current Address: Haverford College, 370 Lancaster Ave., Haverford, PA 19041.

² Current Address: Ecosystems Center, Marine Biological Laboratory, 7 MBL Street, Woods Hole, MA 02543.

Abstract: Pyrite oxidation and NO₃⁻ loading to estuaries present unique environmental problems, however the combination of both processes may present a stronger result than either individually. I studied the effects of NO₃⁻ fertilization on pyrite oxidation in salt marshes with the hypothesis that NO₃⁻ fertilization increases pyrite oxidation. The experiment's design consisted of a long-term, 4-year, fertilization field site from Plum Island Estuary and a short-term, 15-day, fertilization experiment created in the laboratory. Results were achieved by studying sulfur and Fe³⁺ concentrations in sediment and the mass balance of input and output dissolved Fe³⁺, SO₄²⁻, NO₃⁻, and alkalinity concentrations in solutions. The results of most of the data demonstrate an unexpected NO₃⁻ effect, however, nitrification and a SO₄²⁻ effect were also suggested. Better care must be taken when selecting controls for this type of experiment.

Key Words/Phrases: pyrite; pyrite oxidation; Plum Island Estuary; nitrate fertilization; nitrogen loading

Introduction:

The mineral, pyrite (FeS₂), provides a store of sulfur in salt marsh sediments. A measured amount of pyrite is the results of two major processes: new pyrite formation and pyrite oxidation. (Giblin 1988). Pyrite oxidizes in salt marshes by an aqueous reaction with ferric iron (Fe³⁺) or oxygen (O₂) as the oxidizing agents to produce sulfate (SO₄²⁻), ferrous iron (Fe²⁺), and protons (H⁺) according to the following reactions:

1. $\text{FeS}_2 + 14\text{Fe}^{3+} + 8\text{H}_2\text{O} \rightarrow 15\text{Fe}^{2+} + 2\text{SO}_4^{2-} + 16\text{H}^+$
2. $\text{FeS}_2 + \frac{7}{2}\text{O}_2 + \text{H}_2\text{O} \rightarrow \text{Fe}^{2+} + 2\text{SO}_4^{2-} + 2\text{H}^+$

(Williamson et al. 1994).

The H⁺ products lower the resulting pH and alkalinity of the salt marsh, creating a toxic environment for some floral and faunal species intolerant of low alkalinity (Portnoy and Giblin 1997; Giblin 1988).

With growing population and development on Cape Cod without a well-developed sewer system, nitrogen inputs to estuaries, mostly in the form of nitrate (NO₃⁻),

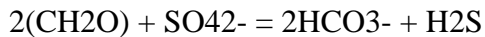
have increased due to septic system outputs and fertilizers from lawns. (Cloern 2001). One of the deleterious results of nitrate inputs is coastal eutrophication, which enhances primary production at the expense of a hypoxic, often deadly, environment for other organisms (Valiela 1995). The focus of this study is to discern whether NO_3^- inputs to salt marshes increase pyrite oxidation.

We expect NO_3^- fertilization to increase pyrite oxidation. We discuss 3 mechanisms by which these results can occur: 1) NO_3^- directly oxidizes pyrite stores in sediment; 2) NO_3^- increases growth of marsh grasses which indirectly oxidizes pyrite stores (Giblin, 1988); and 3) NO_3^- acts as an alternate electron acceptor that inhibits the reduction of SO_4^{2-} to sulfides (H_2S) needed for pyrite formation. (Giblin 1988).

1) A pyrite-oxidation reaction involving nitrate (NO_3^-) as an electron acceptor might be expected due to nitrate's status as a stronger electron acceptor than Fe^{+3} , however, this has been shown not to occur naturally because the microbial communities performing pyrite oxidation are not adapted to use NO_3^- as an oxidizing agent, and the crystal field theory of pyrite is not ideal for a reaction with pyrite. (Taylor et al. 1984; Williamson et al. 1994; unpublished, Vallino 2007; Giblin 2007, pers. comm.). Nevertheless, a growing field of research is directed towards finding correlations between denitrification and pyrite oxidation, which suggests further study of this pathway in the future. (Engesgaard and Kipp 1992)

2) NO_3^- can oxidize pyrite by a more indirect method. Grasses, specifically *Spartina* sp., take up NO_3^- increasing their rooting depth and lowering the water table. (Giblin 1988). Subsequently, O_2 and Fe^{3+} can penetrate to greater depths in the sediment and oxidize more stores of pyrite.

3) Pyrite formation depends on the reduction of SO_4^{2-} to H_2S by the reaction:



(Giblin et al. 1990)

If NO_3^- is used as the electron acceptor, rather than SO_4^{2-} , the rate of new pyrite formation will be inhibited. While this process does not involve pyrite oxidation, it does affect the amount of pyrite stored in sediment, and can therefore be considered a pertinent effect of nitrate fertilization.

Methods

Experimental Design

Salt marshes provide the ideal site to study pyrite because pyrite comprises most of the total sulfur content of the sediments: pyrite and organic sulfur (Giblin et al. 1990; Howarth and Merkel 1984; Berner 1984). I chose to study the effects of NO_3^- fertilization on both long-term and short-term time scales. I chose a site at the Plum Island Estuary, MA (PIE) that had been fertilized with 70 mM NO_3^- over 4 years to study long-term fertilization. (Fig. 1) I extracted cores from Great Sippewissett Marsh, MA (GSM) and treated them with varying NO_3^- and SO_4^{2-} concentrations in the laboratory for 15 days to study short-term fertilization.

For the long-term study, 4 6.5 cm diameter cores were taken at least 20cm deep from *Spartina patens* nitrate-fertilized sediments at Sweeney Creek (Fig. 2), while another 4 6.5 cm diameter cores were also taken from *Spartina patens* sediments at a control site, West Creek (Fig. 3), using the same procedure. Sediment analyses for total

sulfur, Fe³⁺, and percent carbon were prepared by oven-drying, crushing, and homogenizing sediment from various depth intervals of the cores.

The short-term fertilization cores derived from *Spartina alterniflora* peat sediments. 8 15.6 cm diameter cores were extracted for treatment in the laboratory which varied concentrations of NO₃⁻ and SO₄²⁻, and 2 6.2 cm diameter cores were extracted for initial values. The pair of 6.2 cm diameter cores were prepared for sediment analysis according to the same procedure as the PIE cores. The initial observable plant growth on the surface of all cores was cut. The 4 treatments applied to the 6.5cm diameter cores were: artificial seawater without SO₄²⁻ with 10 mM NO₃⁻ in a 101:1 dilution (ASW+NO₃), filtered seawater with 10 mM NO₃⁻ in a 101:1 dilution (SW+NO₃), artificial seawater without SO₄²⁻ (ASW), and filtered seawater (SW). Each of the 4 treatments was added as an input volume that varied from 300 to 500 mL to a pair of replicate cores periodically. The output that percolated through the cores was usually collected the same day as the input. (Table 1). All cores were outfitted with a watertight stopper apparatus on the bottom of the cores to accurately trap the output volume. Filtered samples of the input and output from the cores were measured for concentrations of NO₃⁻, dissolved Fe³⁺, SO₄²⁻, and alkalinity. Only alkalinity measurements were performed the same day that the output was collected from the core. At the end of the 15 day treatment, 4.4cm diameter cores were taken from each treated core and prepared for sediment analysis by the same method as the PIE cores.

Analytical Methods:

Alkalinity was measured using a HACH digital titration of inputs and outputs with 0.16 N H₂SO₄ and pH meter. The nitrate concentrations in the input and output were measured using the Lachat Flow injection analyzer.(Wood et al. 1967). The sulfate and chloride concentrations were measured using the DINEX machine. The concentration of Fe³⁺ in the input, output, and sediment extractions were measured using the model 2380 Atomic Absorption Spectrophotometer (Giblin 2007, pers. comm., Giblin, 1988). Fe³⁺ was extracted from sediment by acidifying 0.1 g sub-samples derived from PIE with 15 mL 5.5N HCl(aq) and 0.1 g sub-samples derived from GSM with 10 mL 5.5N HCl(aq). After vigorous shaking and time to allow the sediment to settle, 1 mL of liquid was removed from the samples, diluted with 9 mL of de-ionized water, and analyzed on the model 2380 Atomic Absorption Spectrophotometer. The total sulfur in sediments was measured using the LECO SC-32 sulfur analyzer by combustion. The percent carbon and nitrogen for the top 8 cm of sediment from the long-term fertilization cores were measured using CHN analysis. All data analysis was conducted using Microsoft Excel, however alkalinity was calculated using the “Alk program for HACH B” spreadsheet designed by A.E. Giblin.

Data Analysis

The results of the input and output for each short-term fertilization core were multiplied by the appropriate conversion and dilution factors to convert to umol/cc. The mass balance, or net output, of concentration in each core was calculated by subtracting the input from the output concentrations. Finally, the mean average and standard error for each pair of replicate cores' values for the net output of each concentration to

determine whether each treatment was retaining or exporting Fe^{3+} , alkalinity, SO_4^{2-} , and NO_3^- .

The concentrations of Fe^{3+} and sulfur in sediments from the long-term and short-term fertilizations were determined by calculating the bulk density, using the dry weight of the sediment divided by the volume of the sediment section. The resulting concentration was multiplied by the measured % sulfur or calculated % extracted iron to determine the concentration of sulfur and iron, respectively, in the sediment section. The appropriate conversions were subsequently calculated to attain the concentration in $\mu\text{mol}/\text{cc}$. The total inventory of Fe^{3+} and sulfur in sediments from the short-term fertilizations was calculated by taking the previously calculated concentration and multiplying it by a specified depth.

Results

Expected Results:

A general trend expected in our results would be to see greater effects of pyrite oxidation occurring in NO_3^- fertilized cores than control cores for both long-term and short-term fertilization. Assuming the effects of NO_3^- extend to 20 cm depth, we would expect higher concentrations of both extracted Fe^{3+} and sulfur in sediment from West Creek than Sweeney Creek throughout the measured depths. If the effects of NO_3^- were unable to penetrate very deep in the sediment, we may only see West Creek exhibiting higher concentrations in the higher depths. We expect to see the % carbon to be lower in fertilized cores than control cores due to the increasing oxidation, or competition for oxidation, of organic compounds with the addition of another electron acceptor, NO_3^- .

Assuming that SO_4^{2-} reduction to H_2S and pyrite oxidation to SO_4^{2-} are the only reactions contributing to alkalinity, a measure of alkalinity should be a fair indicator of net formation or net oxidation of pyrite. A positive net alkalinity suggests net pyrite formation, while a negative net alkalinity suggests net pyrite oxidation. We expect that the NO_3^- fertilized cores, ASW+ NO_3 and SW+ NO_3 , show more negative net alkalinity than the control cores, ASW and SW. We expect that the fertilized cores would retain the added NO_3^- for plant uptake and oxidation, potentially of pyrite, while the control cores would demonstrate the relative rates of nitrification to be considered occurring also in the fertilized cores. Further, the fertilized cores should show more negative net NO_3^- output values than the control cores.

Since no Fe^{3+} , an oxidizing agent for pyrite oxidation, is added to any cores, the net output Fe^{3+} concentration would be expected to be more negative in NO_3^- fertilized cores than control cores because pyrite oxidation would be expected to be occurring faster in fertilized than in control cores. Similarly, we would expect that the Fe^{3+} inventory would show lower values for the fertilized cores than for the control and the initial cores in at least the top 5 cm, where the effects of NO_3^- fertilization would be expected to occur. Similar results from 5-15 cm would confirm our assumption that the NO_3^- effects extend 15cm deep.

The SO_4^{2-} net output results depend on the contributions of two reactions: 1) SO_4^{2-} reduction to H_2S , and 2) pyrite oxidation. An increase in (1) should decrease the output of SO_4^{2-} , while an increase in (2) should increase output of SO_4^{2-} . As a result, the fertilized cores, ASW+ NO_3 and SW+ NO_3 , should show greater net outputs of SO_4^{2-} than their corresponding control cores, ASW and SW, respectively. The net

output of ASW+NO₃ should be the highest of all treatments because little SO₄²⁻ reduction occurs due to the lack of SO₄²⁻ in the input and inhibition by NO₃⁻. In addition, pyrite oxidation should be high as NO₃⁻ is in the input, producing SO₄²⁻. The net output of ASW should be lower than ASW+NO₃ because pyrite oxidation is lower and SO₄²⁻ reduction can occur uninhibited. The net output of SW should be the lowest of all the treatments because SO₄²⁻ reduction is high due to high concentrations of SO₄²⁻ in the input. The net output of SW+NO₃ should be higher than SW because NO₃ will inhibit SO₄ reduction and increase pyrite oxidation, producing more overall SO₄²⁻ than SW.

We expect the sulfur inventory distribution across 4 treatments to show lower values for NO₃⁻ fertilized cores than control cores due to increased rates of pyrite oxidation. In addition, we expect the NO₃⁻ fertilized cores to show less sulfur than the initial sulfur inventory.

Actual Results

The long-term fertilization results demonstrate higher concentrations of sulfur and Fe³⁺ at all depths of NO₃⁻ fertilized compared to control cores, suggesting a NO₃⁻ effect (Fig. 4). The % carbon results from the top 8 cm of depth in the PIE cores show fertilized cores maintaining higher % carbon at surface depths than control cores, while control cores show higher % carbon in sediments at lower depths, suggesting a NO₃⁻ effect (Fig. 5).

The net output alkalinity results were inconclusive, showing no NO₃⁻ effect and no significant SO₄²⁻ effect (Fig. 6). Although ASW+NO₃ showed the highest net

output, SW+NO₃ showed the lowest. A correlation might be inferred from the high net outputs from both ASW treatments, however, both display a lugubrious amount of standard error suggesting insignificant results.

The net output NO₃⁻ results suggest NO₃⁻ net storage in NO₃⁻ fertilized cores and NO₃⁻ net export in control cores, suggesting net pyrite oxidation in fertilized cores (Fig. 7). Both ASW+NO₃ and SW+NO₃ show negative net outputs at a magnitude greater than 200 μmol NO₃⁻, while ASW and SW show positive net outputs of NO₃⁻.

The net output Fe³⁺ results suggest no significant effect of NO₃⁻. (Fig. 8). ASW+NO₃ has a smaller value than ASW, while SW+NO₃ shows a great deal of standard error and has a higher value than SW. All treatments show a net export of Fe³⁺ by their positive net output values, suggesting that net pyrite formation is occurring in all treatments. The Fe³⁺ inventory shows a decrease in all treatments in Fe³⁺ in the top 5cm, supporting the Fe³⁺ net output results (Fig. 9). Although the treatments show a loss with respect to the initial value for 0-5 cm, no consistent trend can be inferred from the 5-15 cm depth data with respect to the initial value. A slight, but significant, NO₃⁻ effect can be interpreted from the Fe³⁺ inventory as ASW+NO₃ and SW+NO₃ show significantly higher values than ASW and SW, respectively. These data suggest that NO₃⁻ fertilization promotes greater rates of net pyrite formation, however, net pyrite formation appears in all treatments.

The net output SO₄²⁻ results suggest little significant effect of NO₃⁻, but do suggest a significant effect of SO₄²⁻ (Fig. 10). ASW+NO₃ and ASW show the only positive net output SO₄²⁻ values, while SW+NO₃ and SW show the only negative net output SO₄²⁻ values. ASW+NO₃ and ASW show approximately the same value, but

ASW+NO₃ has such a high standard error no conclusions can be drawn. SW+NO₃ is much greater in magnitude than SW, suggesting that NO₃⁻ promotes net SO₄²⁻ storage. The positive values for ASW treatments compared to the negative values for SW treatments suggest that SO₄²⁻ promotes pyrite formation and its absence promotes pyrite oxidation. To attain conclusive results on the effect of NO₃⁻ on SO₄²⁻ export or storage, a SO₄:Cl ratio for ASW cores shows no NO₃⁻ effect as both fertilized and control nearly replicate each other's curves (Fig. 11). The sulfur inventory results show no significant NO₃⁻ effect or trends from below 5 cm, but do exhibit an overall loss of sulfur for all treatments with respect to the initial value in the top 5 cm (Fig.12).

Discussion

The long-term fertilization sulfur and ferric iron data can be explained by poor control site criteria and extraction location. We extracted cores from West Creek assuming that the site would represent conditions at Sweeney Creek before NO₃⁻ fertilization began in 2004, however, this assumption was never verified with a comparison of baseline nutrient concentration data from both sites. Although extraction from *Spartina patens* sediments were assumed to show the same NO₃⁻ effects as expected on *Spartina alterniflora* sediments, the *Spartina patens* is sometimes a meter further on the creek bank than the *Spartina alterniflora*, suggesting that some of our sediments may not have been exposed to the NO₃⁻ distributed by tides as expected. The % carbon data suggest that NO₃⁻ effects are more prominent at depth than at the surface because the % carbon decrease with depth suggests that NO₃⁻ and SO₄²⁻ are oxidizing more organic compounds at depth than at the surface.

The alkalinity results can be explained by two processes: mass balance error and nitrification. Although we had been careful to accurately measure all of the output from the cores, often, the cores' stopper apparatus was not as watertight as expected, allowing unaccounted liquid to leak out of the core. Further, the input at any one date never drained entirely, as some input was always retained (Table 1). This fact suggests that the output at any one date is contaminated by the remnants from the previous date's input. We had initially stated that alkalinity would be an accurate determinant of net pyrite oxidation because we assumed SO_4^{2-} reduction and pyrite oxidation to be the only significant reactions influencing alkalinity, however, the oxidation of ammonia to nitrate that occurs in nitrification may be significant enough to release H^+ in solution and affect alkalinity.

The NO_3^- fertilized data can be explained by plant uptake, oxidation, and perhaps denitrification and/or dissimilatory nitrate reduction to ammonium (DNRA), while the control data suggests nitrification. Observations of plant growth on the surface of the NO_3^- fertilized cores suggest that plant uptake is a possible sink of the NO_3^- input. Oxidation of organic compounds by reduction of NO_3^- , releasing unmeasured dinitrogen gas (N_2) and/or ammonium (NH_4^+) in the processes of denitrification and/or DNRA respectively is another possible sink of NO_3^- input. Results from the 4-year long-term fertilization of PIE with 70 mM suggests uptake by the marsh ecosystem, including marsh grasses, lending support to our proposed means of NO_3^- storage (Deegan et al. 2007).

The Fe^{3+} net output data can be explained by the poor mass balance of the cores. The legacy effect of the previous date's input being inaccurately collected in the next

output provides high standard error and blurs the clarity of results. The Fe^{3+} inventory for the top 5 cm shows the opposite of our expected results, which may be explained by our method of Fe^{3+} extraction that measured Fe-oxides. Perhaps Fe^{2+} , a product of pyrite oxidation, in addition to Fe^{3+} is binding with oxygen and being inaccurately measured as Fe^{3+} in our measurements. Regardless, all the treatments show an overall loss with respect to the initial value for 0-5 cm, whereas for 5-15cm depth, no discernible pattern with respect to the initial value can be interpreted.

The SO_4^{2-} net output data provides evidence to suggest that the SO_4^{2-} reduction reaction to H_2S detracts NO_3^- from affecting pyrite oxidation. When SO_4^{2-} is input at a much higher concentration than NO_3^- in SW, its oxidation of organic compounds may challenge the electronegativity of NO_3^- to the organic compounds, causing a stronger attraction between NO_3^- and the organics. The ultimate result of this chemistry causes decreased pyrite oxidation and increased pyrite formation. The sulfur inventory data may not show a NO_3^- effect because the fertilization needs to exceed 15 days to show significant results. Like the iron inventory data, however, effects are most visible in the top 5 cm.

Conclusions:

The long-term fertilization results show an unexpected NO_3^- effect, as the fertilized cores were expected to demonstrate lower concentrations of extracted Fe^{3+} and sulfur than the control, while the opposite was shown in results. The % carbon showed the expected NO_3^- effect, but only from depths of 2-8 cm.

The results of short-term fertilization almost always contradicted our expectations; however, an unexpected NO_3^- effect could be discerned in several portions of data. Our alkalinity data proved inconclusive, due in part to the NO_3^- net output results, which demonstrated nitrification in control cores and NO_3^- net storage in fertilized cores. The Fe^{3+} net output and inventory data support unexpected NO_3^- effect. They suggest net pyrite formation for all treatments, but fertilized cores show greater pyrite formation than control cores. The SO_4^{2-} net output data reject a NO_3^- effect, but introduce the possibility of a SO_4^{2-} effect as SO_4^{2-} promotes net pyrite formation, and lack of SO_4^{2-} promotes net pyrite oxidation. Sulfur inventory data shows no SO_4^{2-} effect or NO_3^- effect, but do suggest net pyrite oxidation in the top 5 cm of all treatments.

If the incubating cores were stressed with high nitrate concentrations over a longer period of time than the 15-day duration of the current treatment, perhaps a clearer NO_3^- effect would emerge. More criteria must be considered when choosing control sites for baseline measurements.

Acknowledgment:

I thank Dr. Anne Giblin, who advised me with every step of my project. I thank the Semester in Environmental Science (SES) program for allowing me to undertake the project. I would also like to thank the SES teaching assistants, Rich McHorney, Will Longo, and Beth Bernhardt for their unending patience and assistance with the project. I thank the Marine Biological Laboratory, and the Ecosystems Center for allowing me to use their facilities and vehicles. I thank Haverford and Bryn Mawr Colleges, especially

Donna Mancini, Jenni Punt, W. Bruce Saunders, Steve Watter, and Arlo Weil, for allowing me to participate in the SES. I thank Ecosystems Center research assistants Aaron Strong and Christina Maki, who assisted me with core extractions from the PIE. Aaron also deserves special thanks for plotting the coordinates of the core extractions using ArcGIS for figures 2 and 3. I thank Linda Deegan for advice and permission to extract cores from her field site. I thank research assistant Sam Kelsey for assistance using the LECO SC-32 sulfur analyzer, and Boston University graduate student Ylva Olsen for assistance running nitrate samples on the Lachat. Lastly, I thank the other SES students for assistance and comraderie.

Appendix:

Table 1: Volumes of input and output and date of collection of short-term fertilization.

Figure 1: Map of Plum Island Estuary, MA showing locations of Sweeney and West Creek. (Deegan et al. 2007)

Figure 2: Map of the fertilized site, Sweeney Creek, in the Plum Island Estuary with sites of core extractions (F1, F2, F3, and F4)

Figure 3: Map of West Creek in the Plum Island Estuary with sites of core extractions (C1, C2, C3, and C4)

Figure 4: Fe³⁺ and Sulfur concentrations at depth for Long-term fertilization results from Plum Island Estuary.

Figure 5: Percent carbon for top 8 cm sediment for Long-term fertilization

Figure 6: Alkalinity net output for Short-term Fertilization

Figure 7: Nitrate net output for Short-term Fertilization

Figure 8: Dissolved Ferric Iron net output for Short-term Fertilization

Figure 9: Iron inventory for Short-term Fertilization

Figure 10: Sulfate net output for Short-term Fertilization

Figure 11: Sulfate:Chloride ratio for ASW cores for Short-term Fertilization

Figure 12: Sulfur inventory for Short-term Fertilization

Table 1

Input (mL)	Date Output	Output(mL)							
	Collected	F1	F2	F3	F4	C1	C2	C3	C4
450	11/18/2007	240	155	0	230	260	200	240	200
450	11/19/2007	280	280	110	90	285	217.5	280	280
300	11/24/2007*	200	100	55	0	165	0	225	235
300	11/25/2007	270	140	155	160	300	90	190	275
500	11/27/2007	470	390	395	435	470	355	440	495
500	11/29/2007	390	430	445	440	455	400	435	425
500	12/2/2007	410	305	425	340	415	385	440	430
500	12/3/2007	410	395	455	340	450	470	420	410

*= Cores were treated with input on 11/20/2007

Table 1. Volumes of input and output and date of output collection for each of 8 cores from the short-term fertilization. The date of collection is the same as the date of input with exception to the 11/24/2007 collection which were treated with input on 11/20/2007. F or C refers to NO₃- fertilized or non-NO₃- fertilized cores respectively. The 1 and 2 cores from both fertilized and control received artificial seawater without SO₄²⁻, while the 3 and 4 cores received filtered seawater containing SO₄²⁻.

Figure 1:

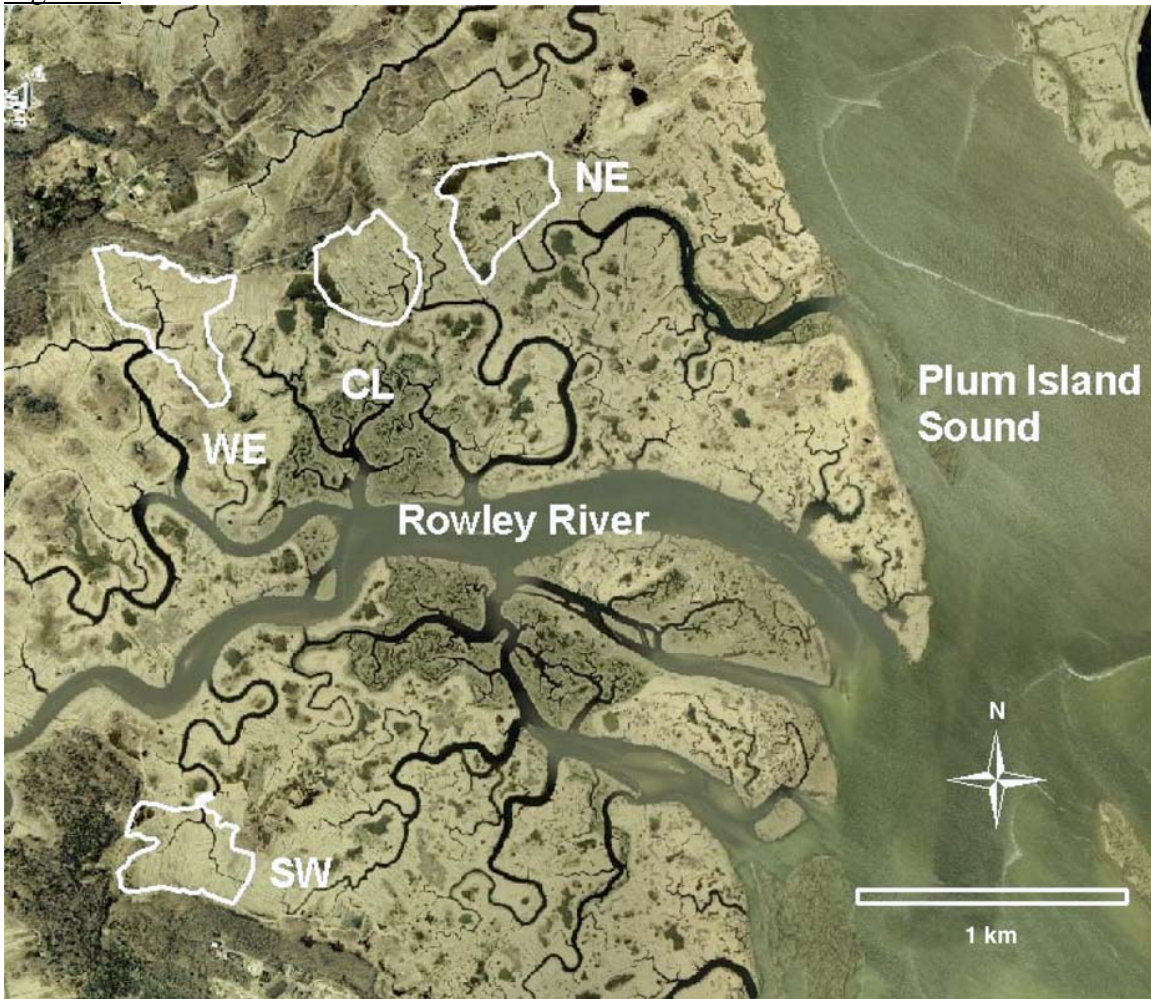


Figure 1. Map of Plum Island Estuary, the long-term fertilization site. SW denotes Sweeney Creek, fertilized site, while WE denotes the control site, West Creek. From Deegan et al. 2007.

Figure 2:

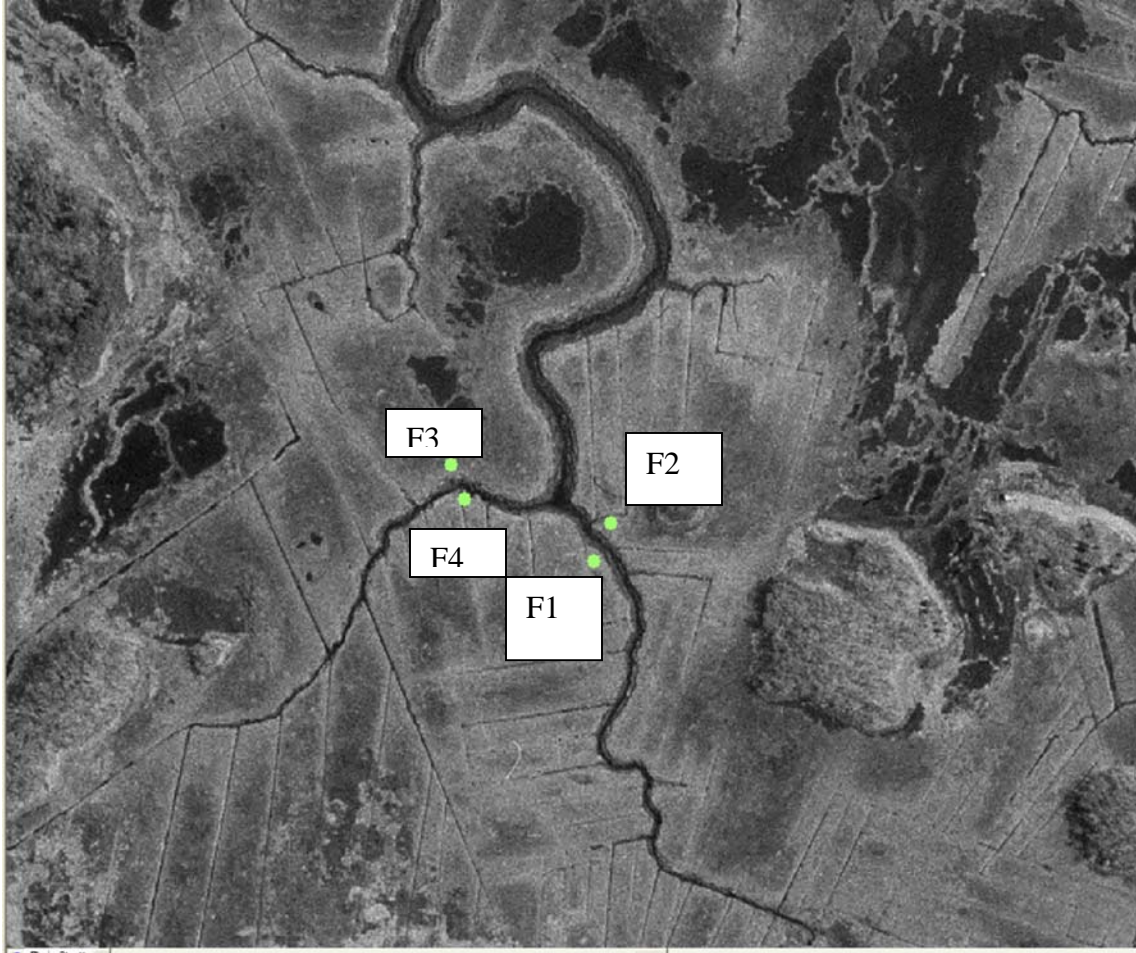


Figure 2. Map of Sweeney Creek, the long-term fertilization fertilized site, with points denoting where 4 core extractions were made. Each point corresponds to a Global Positioning Satellite coordinate measured in the field, which were calculated and compiled using ArcGIS software.

Figure 3

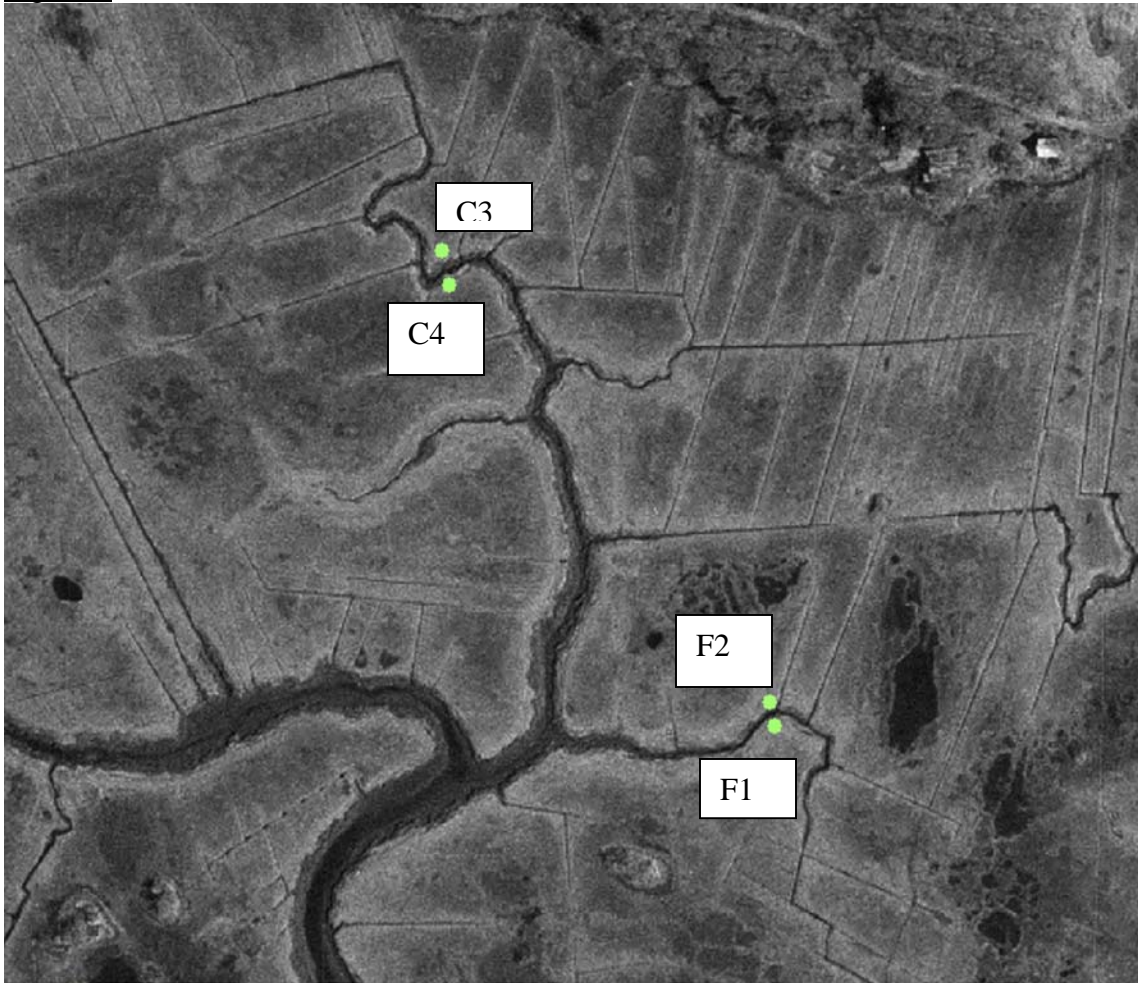


Figure 3: Map of West Creek, the long-term fertilization control site, with points denoting where 4 core extractions were made. Each point corresponds to a Global Positioning Satellite coordinate measured in the field, which were calculated and compiled using ArcGIS software.

Figure 4

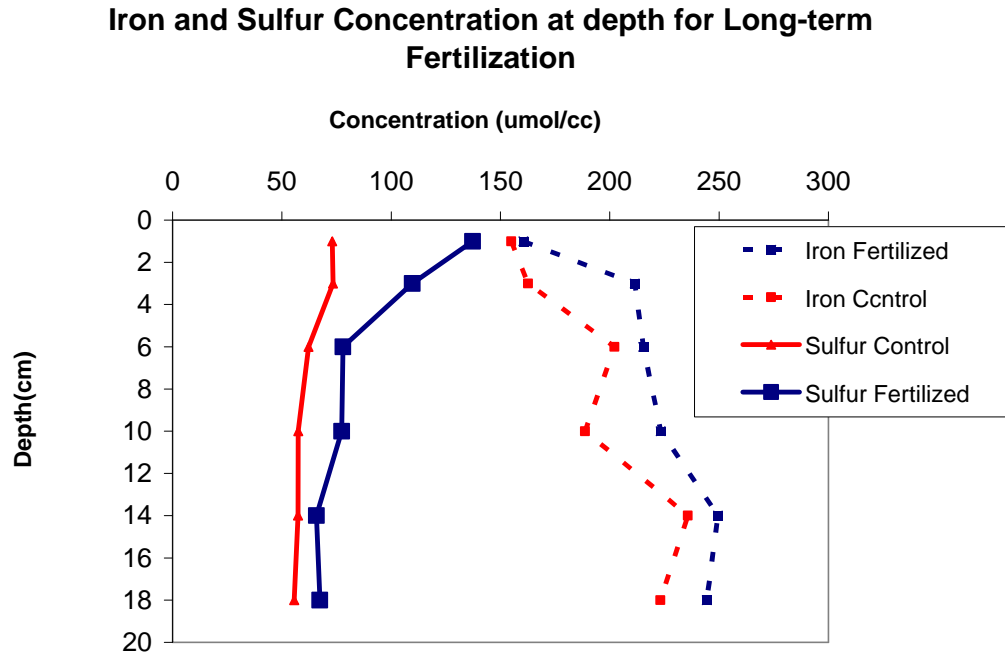


Figure 4. Mean average Fe³⁺ and sulfur concentrations versus depth for 4 fertilized and 4 control cores extracted from *Spartina patens* sediment at Sweeney Creek and West Creek, respectively, at PIE. Each data point represents the midpoint of the depth interval where the sediment derived.

Figure 5

Percent Carbon for top 8 cm from Long-term Fertilization

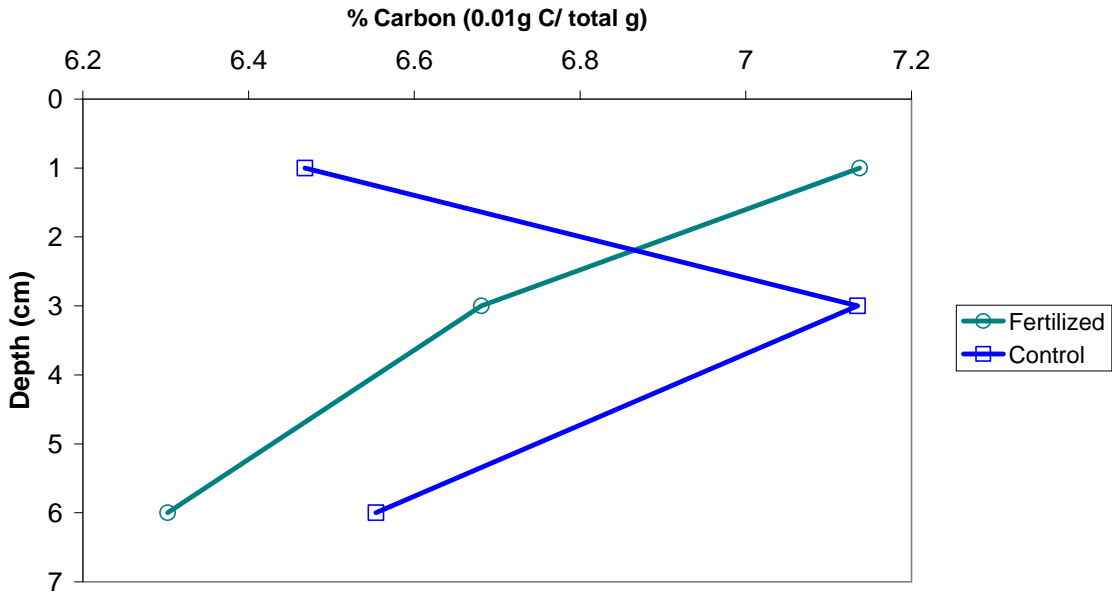


Figure 5. Mean average % Carbon values versus depth for the top 8 cm of 4 fertilized and 4 control cores extracted from *Spartina patens* sediment at Sweeney Creek and West Creek, respectively, at PIE. Each data point represents the midpoint of the depth interval where the sediment derived.

Figure 6

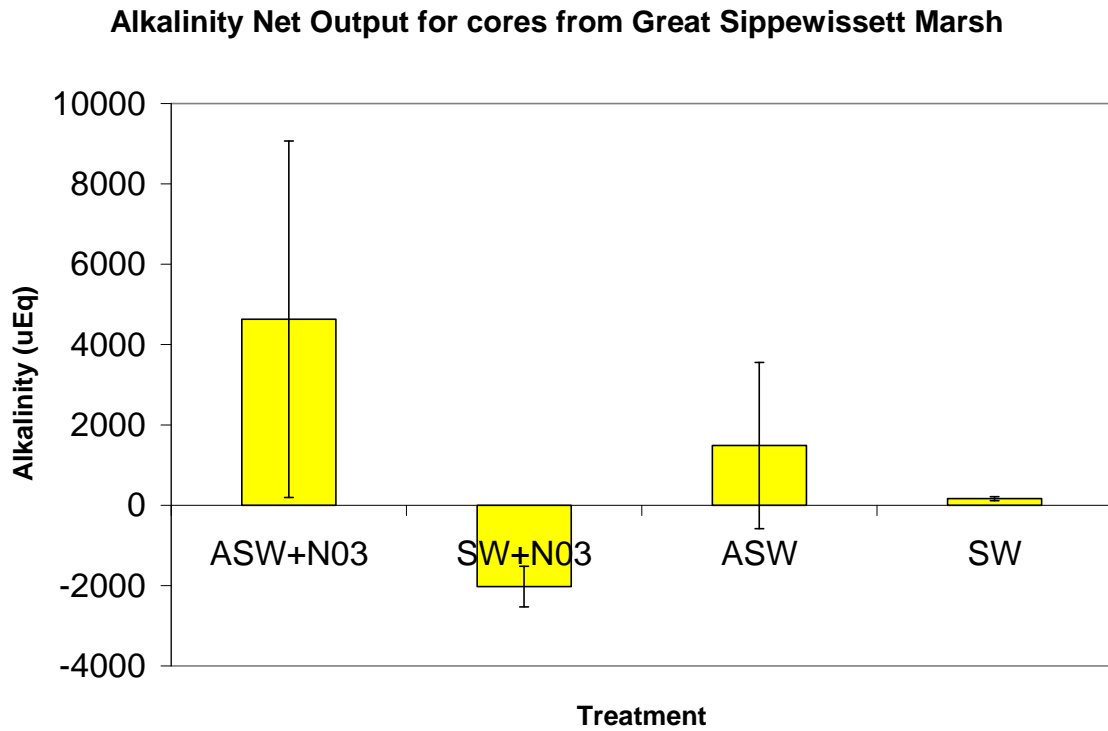


Figure 6. Mean average alkalinity net output and standard error of 2 replicate cores for each of 4 treatments on short-term fertilization cores extracted from Great Sippewissett Marsh treated for 15 days.

Figure 7

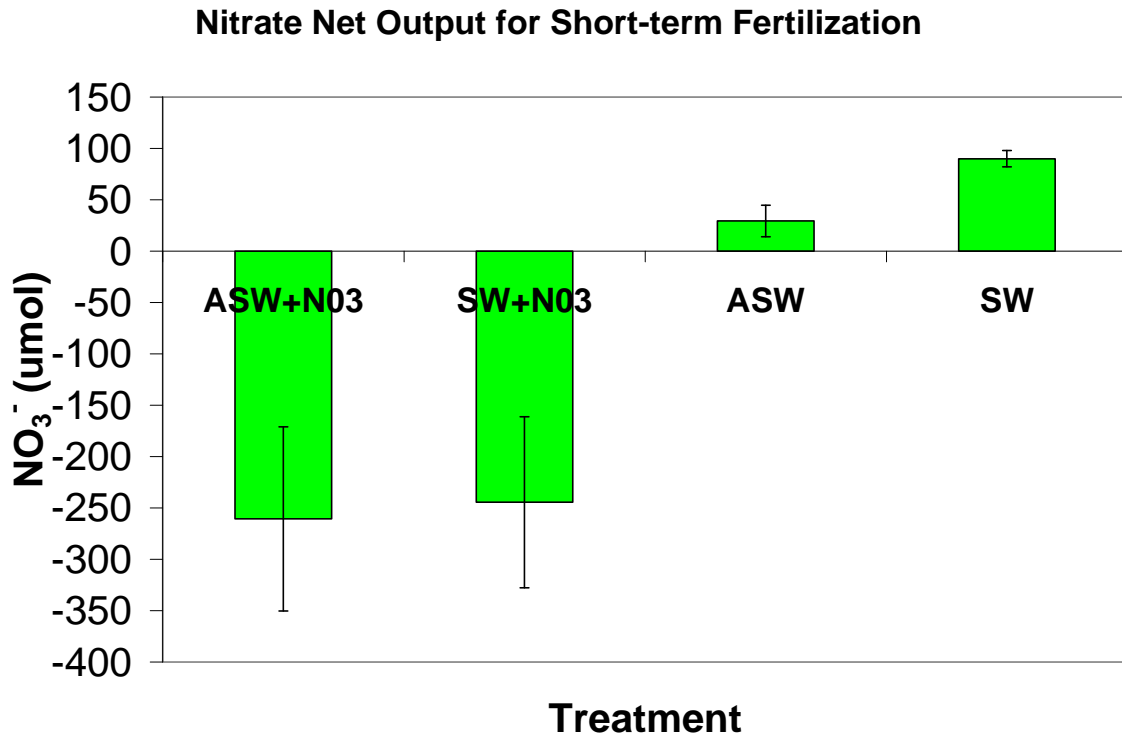


Figure 7. Mean average nitrate net output and standard error of 2 replicate cores for each of 4 treatments on short-term fertilization cores extracted from Great Sippewissett Marsh treated for 15 days.

Figure 8

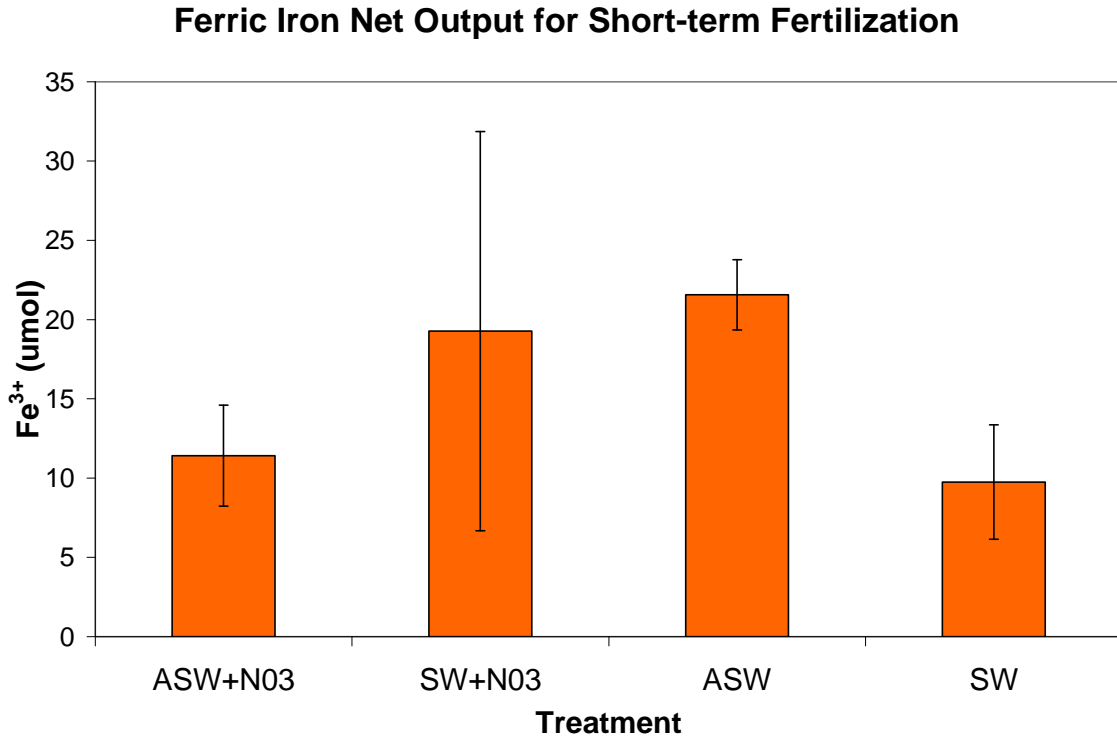


Figure 8. Mean average ferric iron net output and standard error of 2 replicate cores for each of 4 treatments on short-term fertilization cores extracted from Great Sippewissett Marsh treated for 15 days.

Figure 9

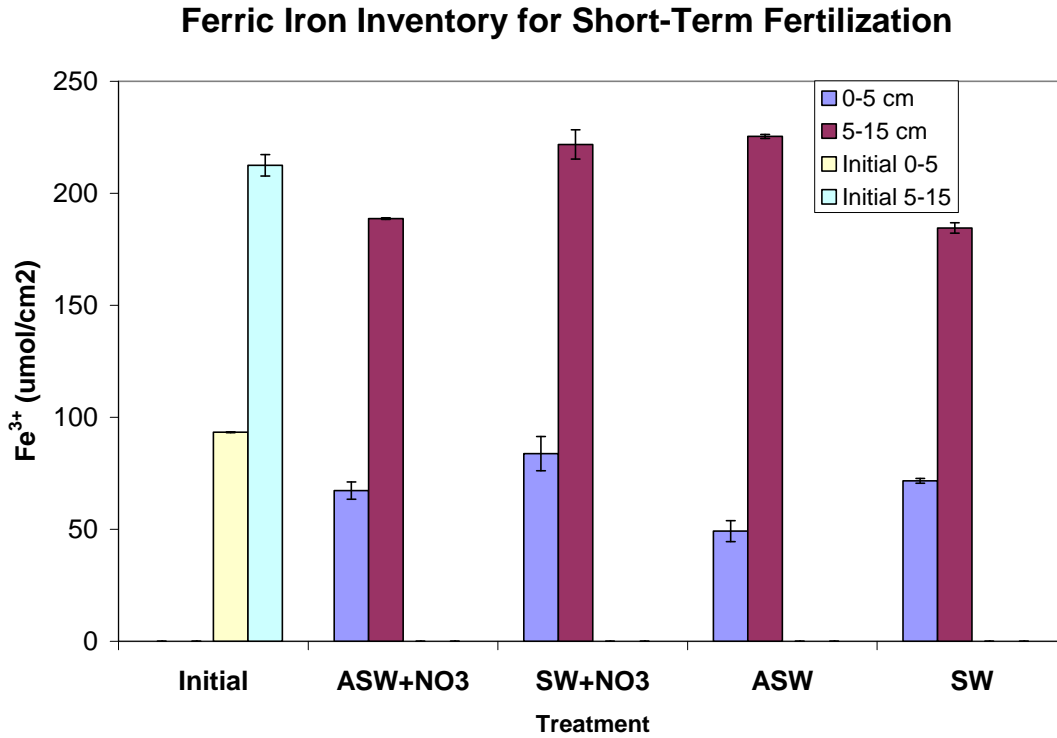


Figure 9. Mean average ferric iron inventory and standard error of 2 replicate cores for initial values and each of 4 treatments on short-term fertilization cores extracted at the end of the 15 day treatment separated into 0-5cm and 5-15cm depths.

Figure 10

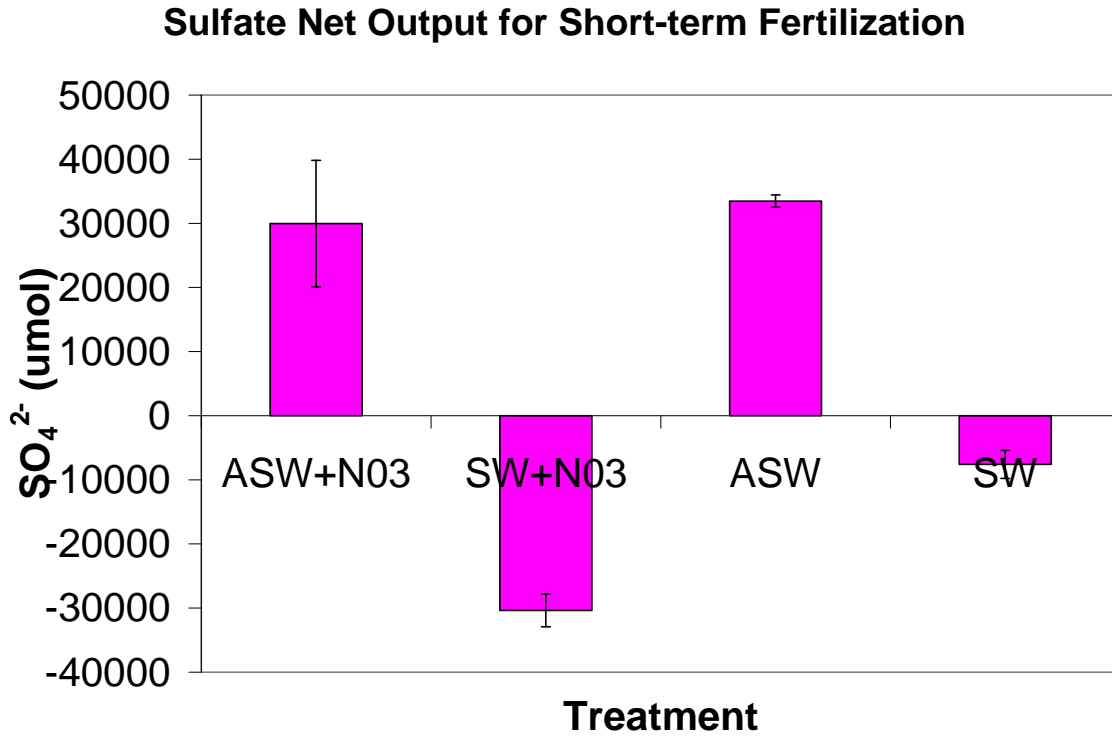


Figure 10. Mean average sulfate net output and standard error of 2 replicate cores for each of 4 treatments on short-term fertilization cores extracted from Great Sippewissett Marsh treated for 15 days.

Figure 11

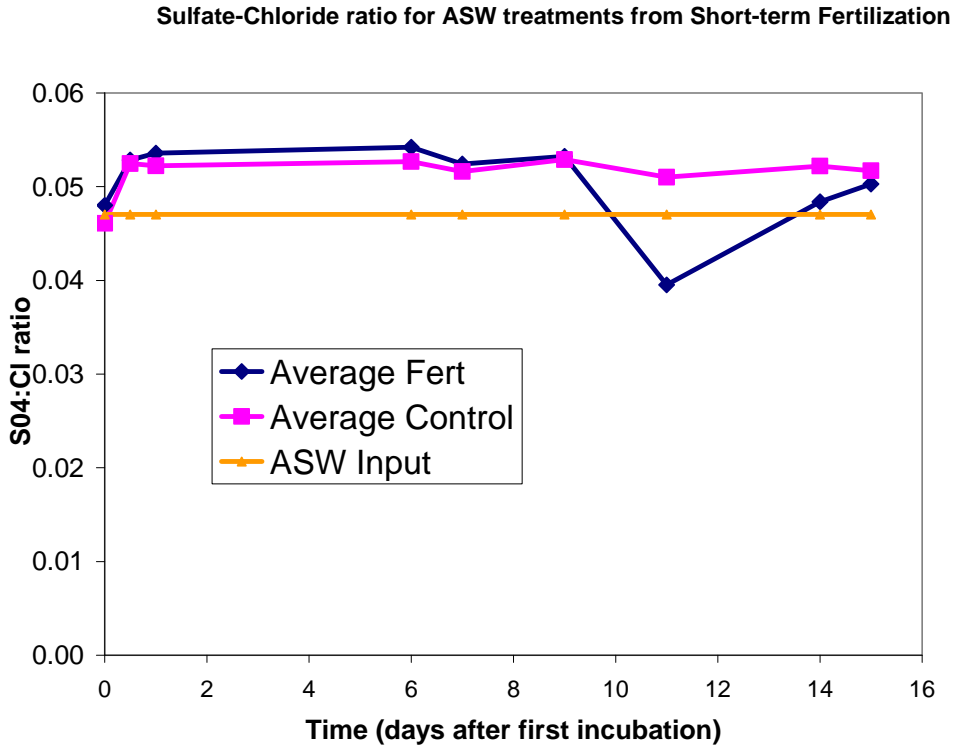


Figure 11. $SO_4^{2-}: Cl^-$ ratio for ASW+NO₃ and ASW compared with the input values of both cores.

Figure 12

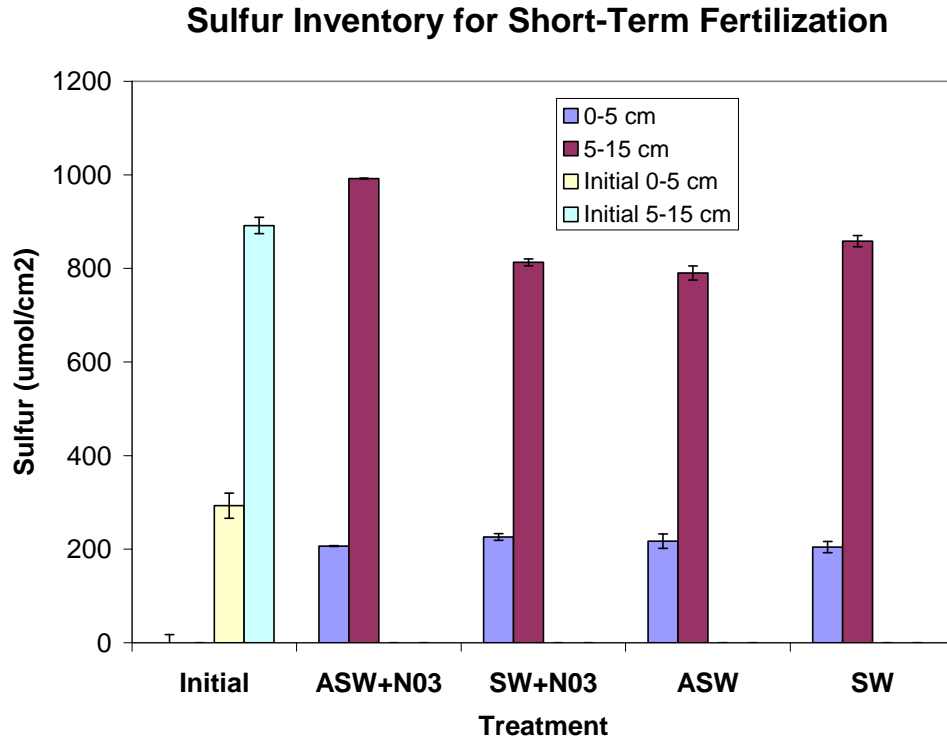


Figure 12. Mean average sulfur inventory and standard error of 2 replicate cores for initial values and each of 4 treatments on short-term fertilization cores extracted at the end of the 15 day treatment separated into 0-5cm and 5-15cm depths.

Literature Cited:

- Berner, R.A. (1984) Sedimentary pyrite formation: an update. *Geochimica et Cosmochimica Acta* 48: 605-615.
- Cline, J.D. (1969) Spectrophotometric determination of hydrogen sulfide in naturwaters. *Limnology and Oceanography*. 14. 454-458.
- Cloern, J. E. (2001) Our evolving conceptual model of the coastal eutrophication problem. *Marine Ecology Progress Series* 210:223–253.
- Dacey, J.W. and B.L. Howes (1984) Water uptake by roots controls water table movement and sediment oxidation in short *Spartina* marsh. *Science*. 287. 487-489.
- Deegan, L.A., Bowen, J.L., Drake, D., Fleeger, J.W., Friedrichs, C.T., Galvan, K.A., Hobbie, J.E., Hopkinson, C., Johnson, S.D., Johnson, J.M., LeMay, L.E., Miller, E., Peterson, B.J., Picard, C., Sheldon, S., Sutherland, M., Vallino, J., and R.S. Warren (2007) Susceptibility of Salt Marshes to Nutrient Enrichment and Predator Removal. *Ecological Applications*. 17:5:42-63
- Engesgaard, P. and K.L. Kipp (1992) A geochemical transport model for redox-controlled movement of mineral fronts in groundwater flow systems: a case of nitrate removal by oxidation of pyrite. *Water Resources Research* 28:10: 2829-2843.
- Giblin, A. (1988). Pyrite Formation in Marshes during Early Diagenesis. *Geomicrobiology Journal*. 6. 77-97.
- Giblin, A.E., Likens, G.E., White, D. and R. H. Howarth(1990) Sulfur storage and alkalinity generation in New England lake sediments. *Limnology and Oceanography* 35:4: 852-869.
- Gilboa-Garber, N. (1971). Direct spectrophotometric determination of inorganic sulfide in biological materials and in other complex mixtures. *Analytical Biochemistry*. 43. 129-133.
- Howarth, R.W. and S. Merkel (1984) Pyrite Formation and the Early Measurement of Sulfate Reduction in Salt Marsh Sediments. *Limnology and Oceanography*. 29:3. 598-608.
- Howes, B.L. Dacey, J.W.H, and G. M. King (1985) Belowground processes in salt marsh sediments: a position paper. Presented at NSF Workshop “A conference on belowground processes in salt marshes,” Feb. 18-19, 1985, Edgewater, MD.
- Portnoy, J.W. and A. E. Giblin (1997) Effects of historic tidal restrictions on salt marsh sediment chemistry. *Biogeochemistry* 36: 275-303.
- Taylor, B.E., Wheeler, M.C., and D.K. Nordstrom (1984) Stable Isotope geochemistry of acid mine drainage: Experimental oxidation of pyrite. *Geochimica et Cosmochimica Acta*. 48. 2669-2678.
- Valiela, I. 1995. *Marine Ecological Processes*. 2nd ed. Springer Science and Business Media, Inc. New York, NY, USA.
- Williamson, M.A. and J. D. Rimstidt (1994) The kinetics of electrochemical rate-determining step of aqueous pyrite oxidation. *Geochimica et Cosmochimica Acta*. 58: 24. 5443-5454.
- Wood, E.D., Armstrong, F.A.G, and F.A. Richards (1967). Determination of nitrate in seawater by cadmium-copper reduction to nitrate. *Journal of Marine Biological Association United Kingdom*. 47:23.